Journal of Sustainable Development of Energy, Water and Environment Systems

http://www.sdewes.org/jsdewes

Year 2025, Volume 13, Issue 4, 1130628

Original Research Article

The Optimal Tilt Angle for Maximizing Energy Production from Bifacial Solar Panels Under Varying Height in Tropical Regions.

Ujah Peter*[1], David Mulati[2], Joseph Ngugi Kamau[3], Timonah Nelson Soitah[4]

[1]Institute of Energy and Environmental Technology, Jomo Kenyatta University of Agriculture and Technology, P.O.BOX 62000-00200 Nairobi, Kenya.

[1]e -mail: petuja4u@gmail.com

[2]Department of Physics, Jomo Kenyatta University of Agriculture and Technology.

[2]e -mail: dmulati@fsc.jkuat.ac.ke

[3]Institute of Energy and Environmental Technology, Jomo Kenyatta University of Agriculture and Technology.

[3]e-mail: ngugikamau@jkuat.ac.ke

[2]Department of Physics, Jomo Kenyatta University of Agriculture and Technology

[4]e -mail: stimonah@jkuat.ac.ke

Cite as: Peter, U., Mulati, D., Kamau, J., Soitah, T., The Optimal Tilt Angle for Maximizing Energy Production from Bifacial solar Panels Under Varying Height in Tropical Regions, J.sustain. dev. energy water environ. syst., 13(4), 1130628, 2025, DOI: https://doi.org/10.13044/j.sdewes.d13.0628

ABSTRACT

Appropriate tilt angle optimization for bifacial solar panels is essential for optimal energy yield since solar incidence angles in tropical low-latitude regions play a significant role in overall performance. The effects of variations in tilt angles 0°, 5°, 10°, and 15° on the components of solar irradiance and energy production are presented here through a combination of simulations and field studies. The study was carried out at Jomo Kenyatta University of Agriculture and Technology, Kenya, at latitude 1.03°S and longitude 36.98°E to assess the effect of tilt angles on the front side beam irradiance and the rear side ground reflected irradiance. Results indicate that while increasing the tilt angle enhances ground reflected irradiance, it leads to beam irradiance losses due to the cosine effect, with reductions of approximately 5 %, 7 %, and 10 % for tilt angles of 5°, 10°, and 15°, respectively. The optimal tilt angle in this study was found to be 5°. The ideal Height was found to be 2 m, where the bifacial panel experienced around 16.8% energy gain. These findings highlight the trade-off between optimizing ground reflection and minimizing angular losses, providing critical insights for the strategic deployment of bifacial PV systems in tropical regions.

KEYWORDS

Optimal tilt angle, Bifacial solar panel, Albedo, Height Variation, Solar irradiance, Cosine effect.

INTRODUCTION

The renewable energy sector is experiencing exponential growth in demand due to the pressing concerns around climate change and fossil fuel dependency. Solar photovoltaics (PV) are key in this transition, particularly in tropical regions, due to abundant solar irradiance. This is particularly relevant for PV plants in this region since their efficiency can be increased mainly by implementing technologies such as solar tracking, which allow more efficient sunlight capture during the day [1]. Solar energy generation is best suited for tropical regions where solar irradiance is very high. Studies have shown that irradiance peaks can reach 850 W/m² within the tropical

* Corresponding author

regions [2]. Technological developments like solar tracking systems have been reported to increase energy production by more than 14% in comparison to fixed systems, since they keep track of the sun's position at maximum irradiation hours [1]. PV systems are a renewable energy source that minimizes greenhouse gas emissions and provides a clean energy alternative for remote communities that are often disconnected from the grid. Despite these benefits, high temperatures and humidity are some of the factors that play a crucial role in the performance of PV modules, and so, specific solutions may be required for tropical climates [3].

Bifacial solar panels absorb Irradiation from both sides, increasing efficiency and energy production in high albedo environments. They can produce up to 30 % more energy than monofacial panels and excel in low-light situations, such as cloudy days [4]. Although bifacial panels are generally more expensive, their higher energy output can lead to reduced land requirements and improved return on investment (ROI). A previous study indicated that replacing a 2.4 MW monofacial system with bifacial panels could reduce the required area by over 27 % while increasing the capacity by 47 % [5]. Advanced maximum power point tracking, therefore, should be further deployed to optimally exploit the output of bifacial panels [6]. Different mounting configurations, like vertical mounting, can improve energy generation profiles as well as decrease soiling effects [7, 8].

Determining the optimal tilt angle and height of the photovoltaic (PV) panels is very important in maximizing energy production, especially in areas with high solar irradiance. The optimal tilt angle varies with location; for example, in Okinawa, Japan, with a latitude of 26.3°, the optimal angle is between 1° and 58° depending on the variation of solar radiation through the year [3]. Fixed tilt angles reduce installation complexity and costs, making them preferable in many scenarios despite the potential benefits of tracking systems [5]. Optimal tilt angle for bifacial PV systems in tropical climates has proven to be a significant research gap, especially regarding different mounting heights [9]. While existing studies have explored tilt angles in different contexts, they often do not consider specific circumstances and ground surfaces common to tropical environments [10]. The installation height of bifacial PV modules has a strong impact on the quantity of light that the rear side receives, which is relevant for its energy production [11].

Studies have shown that the optimum annual tilt angle is similar to the site latitude, as observed in Izmir, Turkey, where it was found to be 35.8° [12]. Different angles have been suggested in other studies, ranging from 10° to 15° [13, 14]. An optimum tilt angle of 30° has been identified for Tehran, which is slightly lower than the city's latitude of 35.7° [15]. The general rule suggests that the optimum tilt angle should be similar to the latitude of the location. Monthly adjustments can yield up to 6.9 % more solar radiation compared to fixed latitude angles [13]. Tilt angle within ±10° is often acceptable, maintaining a relative error of solar energy gain below 1.5 % [14]. In certain locations, such as Ipoh, Malaysia, using the monthly optimum tilt angle can lead to energy production increases of up to 7.96 % [16]. Additionally, a north-south facing tilt could capture more solar radiation for some months of the year [17].

In the assessment of the performance of solar collectors at optimum tilt angles in low latitude regions, specifically Nigeria, with a latitude between 4° and 14°, it was found that there are significant variations across months and seasons. The monthly optimum tilt has been observed to range between 4° and 18.84°, with an average seasonal optimum of 11.24° in the dry season and 8.8° in the rainy season, which translates to an annual optimum tilt of 9.4° [18]. In Kenya, the optimal angles are between 0° and 5° for latitudes between 0.5° to 4.04°, depending on the variation of solar radiation throughout the year [19]. In Uganda, with a latitude of 1.3° to 7°, the annual optimum tilt angle for solar panels ranged from 0° to 5° [20]. In Tanzania (Kilimanjaro) with a latitude of 3°, the annual tilt angle was estimated to be 2° [21]. It is estimated that seasonal adjustment of the tilt angles several times per year can result in 11 % to 18 % higher solar energy collection compared to fixed angles [22]. However, the complexity of frequent adjustments may deter practical implementations [23]. A suggestion for fixed angles was made by some researchers who believe that fixed angles help installation and maintenance, even when energy yields may be lower [24].

The optimum tilt angles have been estimated through the use of mathematical models in various studies based on solar radiation data, thus indicating the necessity for local, specific approaches [25]. The optimum annual tilt angle in Kuala Lumpur is 10° [26]. In Brunei Darussalam is 3.3° [22], and in Sanliurfa, Turkey, the monthly range has a minimum of 13° in June and a maximum of 61° in December [14]. It is known that the optimum tilt angle of PV panels varies according to the specific location, the season of the year and the type of system configuration [27, 28]. Seasonally, the optimum tilt angle for a single bifacial module at 35°N, for a location like Albuquerque, would be 5° in summer and 65° in winter [29]. However, larger systems may require higher tilt angles, up to 20° more than single module systems, due to factors such as horizon blocking and ground shadowing [29, 30]. The results obtained for the optimal tilt angle of bifacial solar panels in tropical regions are crucial for sustainable energy planning. The use of these optimal tilt angles in energy planning can result in a more efficient use of solar energy, especially in urban areas where land space is limited. Therefore, by determining the optimal tilt angles, urban planners will be able to increase energy production without needing more land area, ultimately lowering land use intensity [31].

Previous studies have shown that the mounting height of bifacial photovoltaic panels significantly influences rear-side irradiance and overall energy yield. When panels are installed at lower heights, such as 1 m, the proximity to the ground reduces reflected irradiance and increases shading effects, leading to suboptimal energy production. In contrast, elevating the mounting height to approximately 1.5 m has been reported to moderately enhance energy output by improving rear-side exposure and minimizing shading losses [32]. The Influence of installation conditions, such as mounting height, can enhance additional energy gains substantially by increasing rear-side reflection and reducing shading. Adjustments to height and other parameters like incidence angle modifiers collectively contribute to optimal energy yield [33].

When designing a tilt angle for bifacial PV modules in tropical climates, there is a need to find a compromise between maximizing the ground reflected irradiance and minimizing the angular losses. The combination of using RADIANCE-based ray tracing simulations [29, 30] and field experiments can yield very accurate estimates on how different tilt angles will perform. While in tropical regions, lower tilt angles of 0°-15° might be more appropriate given the high position of the sun, parameters related to the specific location, such as albedo, size of the system, and local climate, should also be taken into account to achieve the best possible energy production [29, 34].

Despite growing interest in bifacial PV technology, there is limited experimental and simulation-based evidence that jointly assesses tilt angle and mounting height optimization in tropical low-latitude settings. In particular, the trade-off between maximizing rear-side reflected irradiance and minimizing cosine effect losses remains poorly quantified for realistic deployment scenarios involving different ground surfaces.

This study addresses the above gap by integrating PVsyst simulations with controlled field experiments to evaluate the interactive effects of tilt angle and mounting height on bifacial PV performance in a tropical environment. By incorporating three distinct albedo surfaces: concrete, sand, and grass, the work provides a comprehensive, location-specific optimization framework that bridges the gap between theoretical modelling and empirical validation for tropical PV deployment.

MATERIALS AND METHODS

A system consisting of three 575Wp bifacial solar panels installed on three different surfaces was deployed to study the impact of varying tilt angles at different heights and compare their performances. The details of these panels are shown in Table 1 and Table 2. The average solar irradiance of approximately 2118 kWh/m² per year was estimated for Kenya. Such high levels of solar radiation make this area very suitable for capturing solar energy, especially bifacial solar technology, since it has the advantage of capturing both direct and diffuse solar radiation [35, 36].

Table 1: Specifications of the bifacial panel

Equipment	Manufacturer	Model	Power	Quantity
Bifacial solar panel	JA	JAM72-D40-575-BP-Bifacial	575W	3

Table 2: Electrical Characteristic of the bifacial panel

Electrical Characteristic	
Power rating	575W
Vmpp	42.88V
Impp	13.41A
Voc	51.40V
Ioc	14.16A
Temperature Coefficient Isc	+0.046%/C
Temperature coefficient Voc	-0.260%/C
Temperature Coefficient Pmax	-0.300%/C

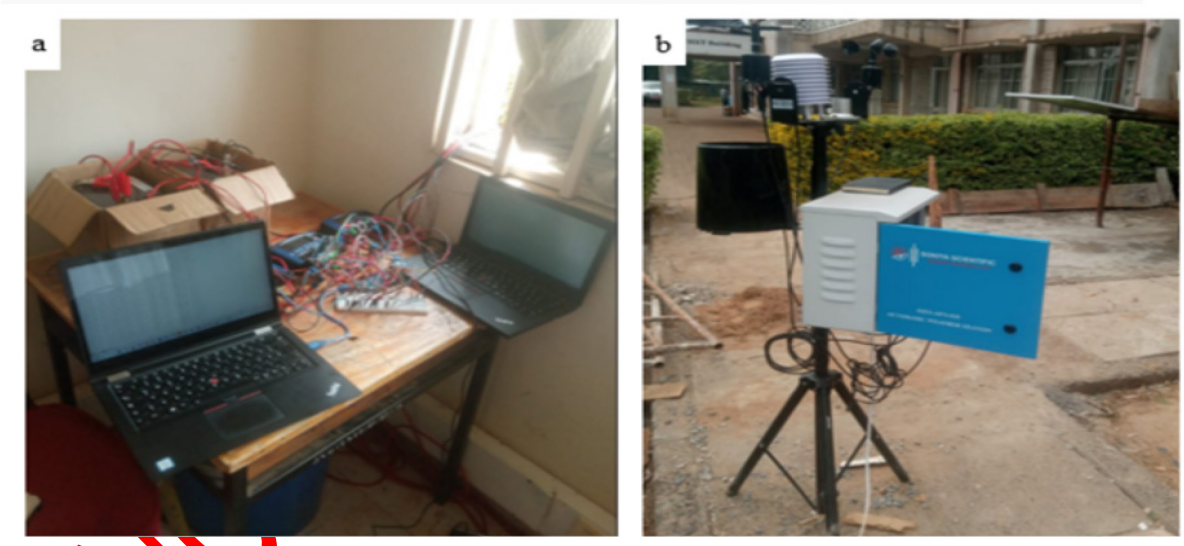

Figure 1: Experimental instrumentation

Figure 1a is the data acquisition system, comprised of computers interfaced with multiple digital sensors and a data logger via wired connections. This setup was used to continuously record electrical output parameters from the bifacial PV modules, including voltage, current, and power. The arrangement ensured high-frequency sampling and real-time monitoring, allowing the detection of short-term variations in performance caused by fluctuating irradiance and environmental conditions. Figure 1b is the automatic weather station, positioned adjacent to the PV test rigs, which was specifically employed to record ambient temperature, which is a key factor influencing PV module efficiency.

Theoretical framework

The solar radiation that reaches a surface in space varies by 63.3 % because of the variation in the distance of the sun to Earth. The amount of extra-terrestrial solar radiation incident on a surface in space at any time of the year can be determined from[37]:

$$I_0 = I_s\left[1 + 0.033\mathrm{Cos}\left(\frac{360N}{365}\right)\right]\mathrm{Cos}\theta_z \quad (1)$$

Where I_0 is the extraterrestrial radiation for a specific day while I_s is the solar constant (1367W/m2), N is the day's number in the year with 1st January as 1, θ_z is the sun's zenith angle.

The extra-terrestrial solar radiation on a horizontal surface per hour was calculated from:

$$I_0 = \frac{12\times3600}{\pi} I_{sc}\left[1 + 0.033\mathrm{Cos}\left(\frac{360N}{365}\right)\right] \times \left[\mathrm{Cos}\emptyset\mathrm{Cos}\delta\,(\mathrm{Sin}H_2 - \mathrm{Sin}H_1) + \left(\frac{2\pi(H_2 - H_1)}{360}\,\mathrm{Sin}\emptyset\mathrm{Sin}\delta\right)\right] \quad (2)$$

Where $\emptyset$ is the latitude of the location, δ is declination, H_1 and H_2 are the hour-angle at 30 minutes before and after the hour under consideration.

The angle of incidence of beam radiation on a horizontal surface, or zenith angle θ_z, can be expressed as [38]:

$$\mathrm{Cos}\theta_z = \mathrm{Cos}\emptyset\,\mathrm{Cos}\delta\,\mathrm{Cos}H + \mathrm{Sin}\emptyset\,\mathrm{Sin}\delta \quad (3)$$

The geometric relationship for the cosine of the angle of incidence of beam radiation on a tilted surface with respect to the horizontal plane can be derived as [39]:

$$\mathrm{Cos}\theta = \mathrm{Cos}\emptyset\mathrm{Sin}\delta\mathrm{Cos}\beta - \mathrm{Cos}\emptyset\,\mathrm{Sin}\delta\,\mathrm{Cos}\gamma + \mathrm{Cos}\emptyset\,\mathrm{Cos}\delta\,\mathrm{CosH}\,\mathrm{Cos}\gamma + \mathrm{Sin}\emptyset\,\mathrm{Cos}\delta\,\mathrm{Sin}\beta\,\mathrm{CosH}\,\mathrm{Cos}\gamma + \mathrm{Cos}\delta\,\mathrm{Sin}\beta\,\mathrm{SinH}\,\mathrm{Sin}\gamma \quad (4)$$

Equation 4 is the cosine effect formula for solar irradiance on a tilted surface. θ is the angle of incidence, the angle between the incoming solar beam (direct normal irradiance) and the normal (perpendicular) to the surface of the bifacial PV panel, H is the hour-angle, γ is the altitude, and β is the slope.

Global horizontal irradiance (GHI) at a given site can be obtained from satellite information, from a weather station positioned in the study site, or from a clear sky model. To find the maximum solar radiation for a given site, the clear sky models are applied to calculate the clearness index [40]. The Kasten-Czeplak (KC) clear sky model for the global horizontal irradiance (W/m²) is given as [41]:

$$\mathrm{GHI} = 9103\,\mathrm{Cos}\theta_z - 30 \quad (5)$$

$$\mathrm{Cos}\theta_z = \mathrm{Cos}\emptyset\,\mathrm{Cos}\delta\,\mathrm{Cos}\,\mathrm{H} + \mathrm{Sin}\emptyset\,\mathrm{Sin}\delta \quad (6)$$

In this work, decomposition models are used to provide accurate estimates of the components [42]:

$$\mathrm{GHI} = \mathrm{DHI} \times \mathrm{Cos}\theta_z + \mathrm{DHI} \quad (7)$$

The model used to calculate irradiance on an inclined plane is the transposition model array. The direct plane of array irradiance can be expressed as [43]:

$$\mathrm{Gd} = \mathrm{DNI}\,\mathrm{Cos}\alpha \quad (8)$$

Where α is the angle of incidence between direct normal irradiance (DNI) and the front/rear side of the solar module. Irradiance transposition was performed using the Perez model, which considers all three diffuse components: isotropic, circumsolar, and horizon diffuse. The reflected irradiance at the ground is described as [43]:

$$GR = GHI \times \rho \times \frac{(1-Cos\theta)}{2} \quad (9)$$

ρ is the albedo, θ is the tilt angle. Albedo refers to the solar radiation that is reflected from a certain surface and is usually expressed in percentages or in a decimal number where 1 is an excellent reflector, like snow or any white surface, while 0 is a surfaces that absorb all incident radiation, like black painted surfaces. Total irradiance on the array plane is expressed as [43]:

$$G_s = G_{bs} + G_{ds} + G_{gs} \quad (10)$$

Where G_s is the sum of all the in-plane irradiance, G_{bs} is the direct normal irradiance, G_{ds} is the sum of the sky diffuse irradiance, and G_{gs} is the sum of the ground reflected irradiance due to the influence of albedo on the plane of an array.

Global Irradiance on the Plane of Array (G_{POA}) as a percentage of Global Horizontal Irradiance (GHI) at each tilt angle provides additional information on the performance of a tilted solar panel as opposed to a horizontal surface, which depends on the tilting angle and orientation. The derived percentage reflects how much irradiance is either gained or lost as a result of the tilt, which can also be useful to determine the effect of the cosine effect and possibly maximize energy yield by adjusting the panels accordingly. To calculate the percentage of G_{POA} relative to GHI for each tilt angle, it can be expressed as:

$$Percentage = \left(\frac{G_{POA}}{GHI}\right) \times 100 \quad (11)$$

The effect of albedo is considerably different for concrete, sand, and grass surfaces, as concrete reflects the most radiation, sand is intermediate, and grass reflects the least. These differences in surface reflectivity have important implications in local as well as global radiative forcing with respect to climate and the Earth's energy balance. The total irradiance received by the plane can be expressed as [44]:

$$G_T = G_{POA} + (BF \times G_{rear}) \quad (12)$$

Where G_{POA} is the incident radiation received on the panel, BF is the bifaciality factor (0.8), and G_{rear} is the reflected irradiance.

For a more rigorous quantitative comparison between the simulation outputs and field measurements, three statistical performance indicators were employed: Mean Absolute Relative Error (MARE), Mean Percent Error (MPE), Mean Absolute Error (MAE), and correlation (r). The MARE expresses prediction errors as a percentage of absolute values between simulated and experimental values, thereby providing a normalized measure of overall accuracy. It is useful for applications involving data with varying scales [45].

$$MARE = \frac{1}{n}\sum_{l=1}^{n}\left|\frac{X_{Exp}-X_{Sim}}{X_{Exp}}\right| \times 100 \quad (13)$$

X_{Exp} is the experimental result, X_{Sim} is the simulated value, n is the number of data point. The MPE quantified the bias in the simulation results, indicating whether the model systematically overestimated or underestimated the experimental values. This quantification is essential for improving model accuracy and predictive capability, as it allows for the identification of systematic errors.

$$\text{MPE} = \frac{1}{n}\sum_{l=1}^{n}\left(\frac{X_{Exp}-X_{Sim}}{X_{Exp}}\right)\times 100 \quad (14)$$

Mean Absolute Error (MAE) measures the average magnitude of errors between simulation and experimental values, without considering the direction (positive or negative). MAE shows the typical size of the errors in the same units as the measurement [45].

$$\text{MAE} = \frac{1}{n}\sum_{l=1}^{n}\left|X_{Exp} - X_{Sim}\right| \quad (15)$$

During comparison, we identified a reporting mismatch between the simulated and measured datasets. The field experiment recorded DC energy aggregated over the array (the summed DC output from the modules), whereas the simulation output files reported AC energy per simulation unit. To ensure a consistent comparison, the simulated AC values were converted to comparable DC totals by accounting for the inverter conversion of 95% as used in the simulation and the photovoltaic panel size used in the experiment. Specifically, simulated AC energy was converted to DC equivalent energy:

$$E_{DC,Sim} = \frac{E_{AC,Sim}-N_{Mod}}{\eta_{Inv}} \quad (16)$$

N_{Mod} is the number of modules represented and η_{Inv} is the inverter efficiency used in the simulation setup.

Equation 17 is a standard approximation used in solar PV performance modelling. It's a key part of the process for adjusting a simulated solar irradiance value to account for real-world losses that are not typically included in the raw simulation.

$$GPOA_{Adj} = \bar{S} \times I\bar{A}M\left(1 - f_{soiling}\right) \times GPOA_{Sim} \quad (17)$$

Where $GPOA_{Adj}$ is the adjusted GPOA, $\bar{S}$ is the average spectral mismatch factor, $I\bar{A}M$ is the average incidence angle modifier, $\left(1 - f_{soiling}\right)$ is the soiling loss factor, and $GPOA_{Sim}$ is the simulated GPOA.

Simulation set-ups

The simulation for the bifacial photovoltaic (PV) system was conducted using PVsyst 8.0.5. The system was modelled for the IEET Building at Jomo Kenyatta University of Agriculture and Technology (JKUAT), Kenya, using synthetic meteorological data from Meteonorm 8.1 (1991–2007). The geographical parameters included a latitude of 1.03°S, a longitude of 36.98°E, and an altitude of 1571 m. The PV system design consisted of an unlimited shed configuration with a tilt and azimuth of 180° South, a height above ground of 1m,1.5 m, 2 m, and 2.5 m, and a ground coverage ratio (GCR) of 30.4 %. A single bifacial module (JAM72-D40-575-BP-Bifacial) with a nominal power of 575 Wp was connected to a single-phase inverter (AS-IR02-700, 0.7 kW, 1 MPPT), resulting in a DC/AC ratio of 0.82. The bifacial model employed was the 2D unlimited sheds configuration, incorporating a bifaciality factor of 80 %, a ground albedo of 0.23 for concrete, 0.21 for sand, and 0.19 for grass. The rear-side shading and mismatch losses are 5 % and 10 %, respectively. The simulation was modelled for the period from February to March. The average ambient temperature was 21.27°C. The energy production was based on the orientation of the panel and the height above the ground. The result from the simulation is presented in Figure 3.

Table 3: Simulation result

Height (m)	Tilt angle(°)	Concrete (kWh)	Sand (kWh)	Grass (kWh)	GHI (W/m²)	GPOA (W/m²)
1	0	12.78	12.74	12.68	785.6	785.6

1	5	12.73	12.67	12.62	785.6	741.9
1	10	12.61	12.55	12.49	785.6	728.9
1	15	12.42	12.36	12.29	785.6	714.1
1.5	0	12.96	12.89	12.83	785.6	785.6
1.5	5	12.88	12.83	12.76	785.6	741.9
1.5	10	12.76	12.69	12.62	785.6	728.9
1.5	15	12.57	12.49	12.42	785.6	714.1
2	0	13.08	13.02	12.95	785.6	785.6
2	5	13.02	12.95	12.86	785.6	741.9
2	10	12.88	12.80	12.73	785.6	728.9
2	15	12.68	12.59	12.52	785.6	714.1
2.5	0	13.16	13.07	13.00	785.6	785.6
2.5	5	13.07	12.98	12.92	785.6	741.9
2.5	10	12.94	12.85	12.77	785.6	728.9
2.5	15	12.73	12.64	12.55	785.6	714.1

Field Set-up

The field setup was designed to be a direct replica of the simulation environment, ensuring the accurate validation of the modelled results. Three types of ground surfaces: concrete, sand, and grass, were prepared, ensuring uniform and even surfaces to minimize variability in measurement. As shown in Figure 2, metallic mounting frames were subsequently mounted on each of the prepared surfaces. As for the orientation, the panels were installed in the north/south direction, as this is the ideal orientation for the location of the study. The mounts were adjustable for tilt angles and had a locking mechanism. More specifically, they were designed to allow for four discrete angles of inclination: 0°, 5°, 10°, and 15°, and performance could thus be measured under varied incline conditions. The mounting structure heights were 1 m, 1.5 m, 2 m, and 2.5 m. A Suunto inclinometer was used for all installations and adjustments in incline angle to ensure that each panel's experimental tilt angle was set accurately.

Figure 2: Image of the bifacial panel mounted on different surfaces.

Thermocouples were installed on the front (top) as well as the back sides of the panels to measure the actual cell temperatures during the tests. Ambient temperature was also recorded throughout the testing period to evaluate environmental influence on panel performance. Each panel configuration was separately connected to one of three MPPT charge controllers, which

directed the power into the 24V 40Ah battery configuration (two 12V 40Ah batteries connected in series). The system load consisted of a 24V 10A DC water pump, which was connected across the terminals of the battery. A data logger was used to log energy generation and energy consumption at 20-second intervals for six hours daily to record the energy performance of the system. Incident and reflected solar irradiance were measured with a TM-208 solar power meter to evaluate the contribution of rear-side gains from bifacial panels. The results of all experimental data are summarized in Table 4, which illustrates system performance.

Table 4**:** Data from the field test

Height (m)	Tilt Angle(°)	Concrete (kWh)	Sand (kWh)	Grass (kWh)	Load (kWh)	GPOA (W/m²)	GHI (W/m²)	RCon (W/m²)	RSand (W/m²)	RGrass (W/m²)
1	0	12.6	12.6	12.4	36.8	890.2	890.2	191.5	173.2	164.6
1	5	12.4	12.4	12.2	36.7	871.9	919.2	189.3	174.1	169.9
1	10	12.1	11.8	11.7	35.1	876.0	954.1	190.0	173.3	168.6
1	15	11.6	11.6	11.4	34.2	826.9	926.0	184.3	171.6	167.7
1.5	0	11.9	11.9	11.7	35.9	637.7	637.7	136.6	124.8	120.9
1.5	5	13.9	13.8	13.6	36.8	801.7	851.0	144.2	131.1	124.8
1.5	10	11.5	11.2	11.1	33.2	503.1	545.1	110.1	102.7	98.0
1.5	15	12.5	12.3	12.2	35.9	565.8	618.2	119.5	110.5	106.2
2	0	14.8	14.7	14.6	36.8	949.9	202.9	191.3	182.2	202.9
2	5	14.6	14.3	14.2	36.5	845.5	212.0	196.7	194.7	212.0
2	10	14.0	13.8	13.8	36.3	724.9	765.1	146.7	135.1	132.4
2	15	13.5	13.3	13.3	36.1	504.2	543.3	109.4	100.4	97.5
2.5	0	14.8	14.7	14.6	36.6	885.3	885.3	185.5	171.1	166.1
2.5	5	14.4	14.2	14.1	36.4	888.3	932.3	181.1	168.1	163.4
2.5	10	13.9	13.5	13.4	36.4	846.8	917.0	190.4	185.4	175.3
2.5	15	11.9	11.7	11.6	35.7	637.3	702.0	129.7	118.8	115.8

In line with the objective of this study, the data collected from the field experiments encompassed key parameters essential for evaluating the performance of bifacial photovoltaic panels under varying tilt angles and mounting heights. Specifically, measurements included the energy harvested from each panel, which served as a direct indicator of system output across different configurations, as shown in Table 4. Solar irradiance data, both incident and reflected, were captured using a solar power meter to assess the total radiation received by the panel surfaces.

RESULTS AND DISCUSSION

Based on the experimental setup, the results obtained, as presented in Table 4, were analysed to determine how varying tilt angles influence the performance of bifacial PV at different heights.

Effect of Tilt Angle

Table 5 presents experimental results showing how varying tilt angles (0°, 5°, 10°, and 15°) affect the Global Horizontal Irradiance (GHI) and Global Plane of Array Irradiance (G_{POA}), along with the percentage of irradiance captured on the panel surface. When the tilt angle of the bifacial solar panels increases, the incident radiation received on the panel surface progressively declines. While the tilt angle varied from 0° to 5°, 10°, and 15°, the incident radiation decreased by approximately 5 %, 7 %, and 10 %, respectively. This decrease in G_{POA} is due to the Cosine effect. Overall, the data suggest that tilt angles between 0° and 5° are optimal for maximizing irradiance capture in fixed PV installations, especially in regions with high sun angles, while larger tilt angles lead to reduced energy captured. The 5° tilt offers practical benefits such as improved self-cleaning. The optimal tilt angle for bifacial PV panels in tropical regions typically ranges from 0° to 15°,

showing improved energy output [2, 46, 47]. In tropical regions where the sun is generally high in the sky, flatter orientations (lower tilt angles) align more directly with the sun's position throughout the day, resulting in greater solar exposure and subsequently higher energy yield [48].

Table 5: The incident irradiation from the experimental result.

Tilt Angle (°)	GHI (W/m²)	G_{POA} (W/m²)	Percentage %
0	841.5	841.5	100
5	902.1	851.1	94.3
10	795.3	737.6	92.7
15	697.4	633.5	90.8

The corresponding beam irradiance from the simulated result is shown in Table 6:

Table 6: The incident irradiation from the Simulation result

Tilt Angle (°)	GHI (W/m²)	G_{POA} (W/m²)	Percentage %
0	785.6	785.6	100
5	785.6	745.8	94.9
10	785.6	730.9	93.1
15	785.6	715.7	91.1

The GHI represents the total solar radiation received per unit area on a horizontal surface and serves as a baseline for estimating available solar energy at a site. However, what the panel absorbs depends heavily on its tilt and orientation. The irradiance on the plane of the bifacial panel (G_{POA}) declined with increasing tilt, despite GHI values remaining stable or only slightly fluctuating. This discrepancy can be attributed to the angular mismatch between the solar beam and the tilted surface.

The simulated GPOA values were adjusted to a real-world equivalent for accurate comparison with experimental data, a standard procedure in solar energy research to account for optical losses not captured in raw simulation outputs. This methodology is based on a conceptual framework that incorporates key loss mechanisms. The incidence angle modifier (IAM) was applied to account for the reduction in performance as sunlight strikes the panel at a non-normal angle, a principle well-established by Duffie and Beckman [49]. Soiling losses, a significant real-world factor, were modeled using a soiling factor derived from the [50] model. The spectral mismatch factor, which accounts for the difference between the simulated and real-world solar spectrum, was also applied, consistent with research and datasets provided by institutions like Sandia National Laboratories [51]. By integrating these validated loss models, the simulated data were converted into a realistic representation, allowing for a robust and meaningful comparison with the experimental field measurements.

To calculate the percentage of G_{POA} relative to GHI for each tilt angle, as shown in Table 5 and Table 6, Equation 11 was used.

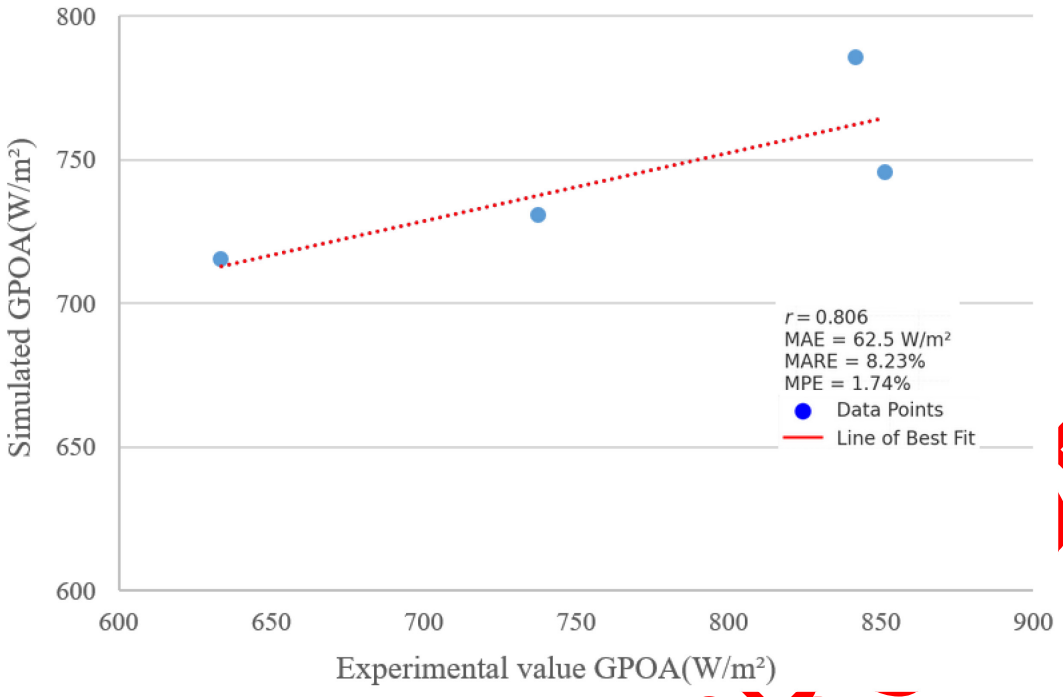

Figure 3: A plot of Simulated value against Experimental value

In this analysis, the performance of a simulation model against experimental data was visually and quantitatively evaluated. As shown in Figure 3, a strong positive linear relationship is evident between the simulated and experimental values, with data points clustering closely around the line of best fit. This visual observation is corroborated by the calculated Pearson correlation coefficient (r = 0.806), which, being very close to the ideal value of 1, indicates that the two datasets change in a highly consistent and predictable manner. While the correlation is strong, a more detailed understanding of the model's accuracy is provided by the error metrics. The Mean Absolute Relative Error (MARE) of 8.23 % indicates that, on average, the simulated values deviate by about 8 % from the actual experimental values, which is below the 10 % threshold commonly cited in photovoltaic performance validation [52]. The Mean Percentage Error (MPE) of 1.74 %, indicates that the simulation slightly underestimates the experimental GPOA values by less than 2 % on average, which is within the ±5 % tolerance defined in ASHRAE Guideline 14 [53]. The Mean Absolute Error (MAE) was found to be 62.5 W/m², corresponding to approximately 6–8 % of typical tropical irradiance values (800–1000 W/m²), which is acceptable given natural sensor uncertainties and environmental variability. Collectively, these results demonstrate that the simulation model provides a highly reliable representation of the experimental trends, with only modest deviations at the individual data-point level.

a

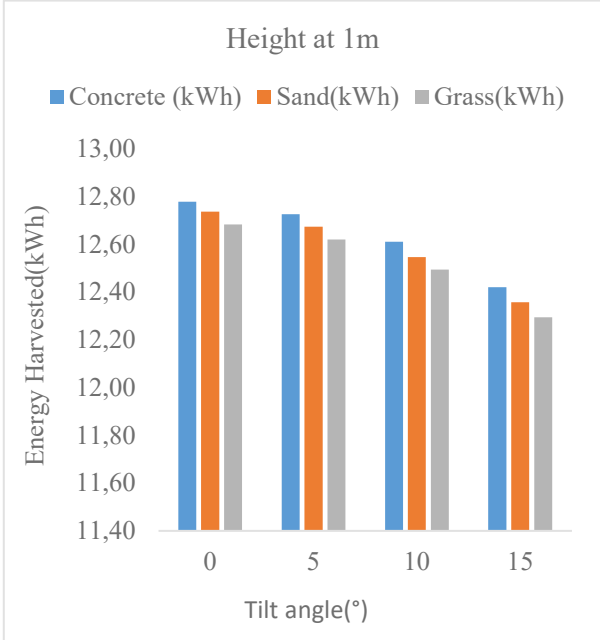

a′

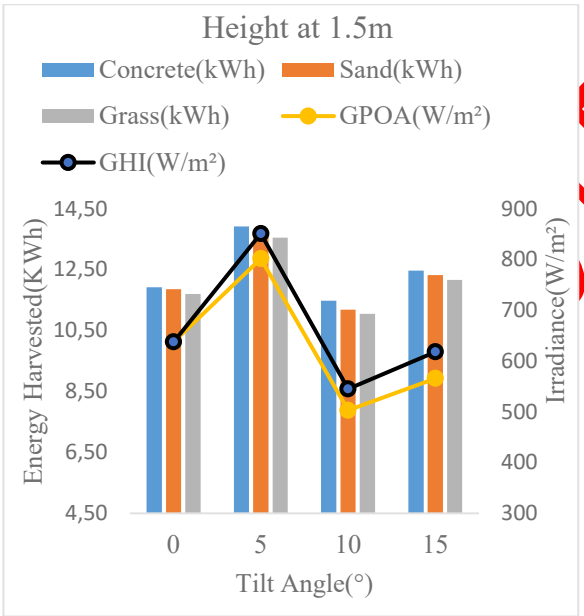

b

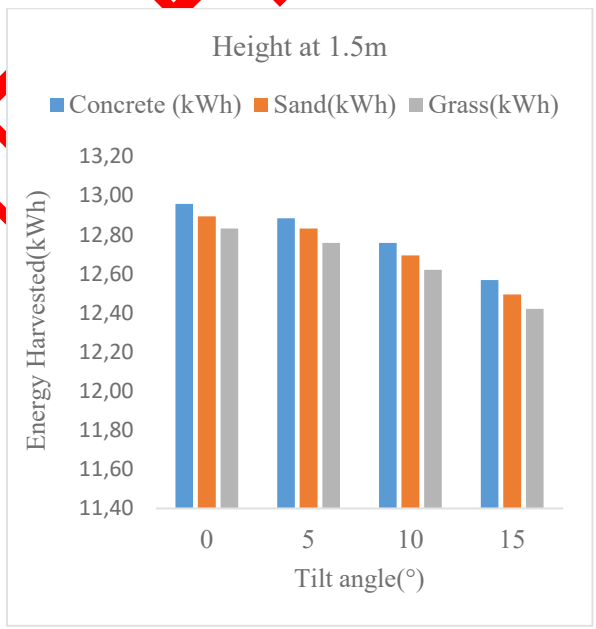

b′

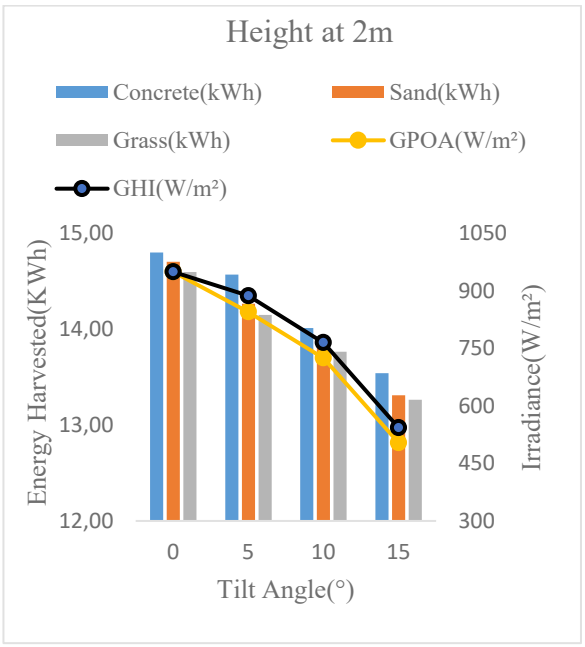

c

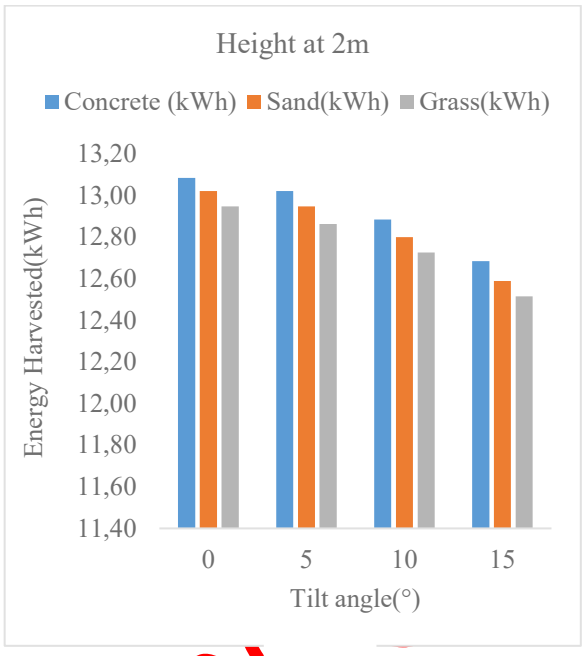

c′

d

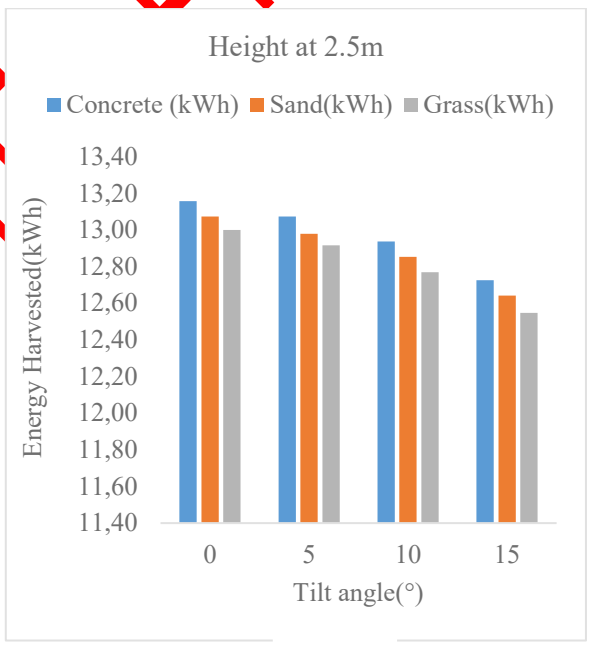

d′

Figure 4: The graph of energy harvested, GHI, and G_{POA} against the varying tilt angle and height.

Figure 4 shows that energy harvested and irradiance (GHI and G_{POA}) vary with tilt angle and installation height across different surfaces in both experimental and simulated setups. Figure 4a, 4*b*, 4c and 4*d* are the results from the experimental results, while the corresponding Figure 4*a′*, 4*b′*, 4*c′* and 34 are from the simulated results at varying heights. At 1m, concrete yields slightly more energy than grass and sand, with high GHI but fluctuating G_{POA}. At 1.5 m, both energy and irradiance increased, indicating minimal shading. The highest energy output occurs at 2 m with 0° to 5° tilt, beyond 5°, both GHI and energy declined. Radwan *et al* [54] reveals that increasing the tilt angle beyond 5° results in reduced GHI and energy output due to less effective rear-side

irradiance capture. At 2.5 m, energy decreases notably at higher tilts despite good irradiance at lower angles.

Results from the field were in accordance with predictions derived from simulation models, thus confirming the theoretical basis of the analysis. Based on the simulation outputs, higher tilt angles would imply a lower total irradiance on the panel's plane because of an apparent misalignment with the sun's trajectory [33]. This prediction was confirmed in the field test, where actual energy harvested decreased with the decrease in incident radiation. These findings highlight that while some tilt can enhance rear side irradiance capture (due to improved reflectance geometry), this gain is overshadowed by the loss in front side irradiance at higher tilt angles [9]. Thus, the field data support the argument that smaller tilt angles are preferred for equatorial climates when maximizing energy capture is the main goal.

The tilt angle of the bifacial solar panels is a determining factor of the energy yield for this current study. Given that solar radiation is time and location-dependent, it is important to improve the tilt angle of the bifacial panels to achieve the most efficient capture of solar energy [27, 28]. Although the use of dynamic sun tracking systems represents the possibility of constantly optimizing the orientation of the panels throughout the day, these have the disadvantage of typically being quite expensive and the complexity to the system. Considering these constraints, the present study looks into another alternative of applying a more practical and feasible solution for actual installations and optimal fixed tilt angle.

Figure 4 is a Comparison of simulated and experimental daily energy yield (kWh) of the bifacial PV array under three different ground surfaces (Concrete, Sand, Grass). The dataset of the simulated result shows an apparent discrepancy of approximately 14. This was due to two issues: (i) The simulation results were reported in AC terms (including inverter efficiency ~95%) while the experimental values were logged in DC. The data was converted to DC using Equation 16 for proper comparison. (ii) the experimental setup was constrained by a fixed resistive load of 24 V × 10 A (≈240 W), corresponding to ~14% of the 1.725 kW array's potential capacity. After harmonizing both datasets to the same DC basis and array scaling, the simulation (~12.8 kWh/day) and experimental (~13 kWh/day) values show close agreement, with residual deviations attributable to wiring/mismatch losses, sensor tolerances, and environmental variability.

Effect of Albedo

Figure 5 shows that the reflected irradiance from different surfaces (concrete, sand, and grass) varies with the tilt angles and height. Among the surfaces, the concrete surface (RCon) consistently reflects more irradiance than sand (RSand) and grass (RGrass) across all tilt angles. The highest reflected irradiance from all surfaces is observed at a tilt angle of 5°, where RCon is slightly above 200 W/m², followed by RSand and RGrass. The lowest values of reflected irradiance occur at a tilt angle of 15°, where all surfaces drop to approximately 97 W/m². This pattern indicates that surface material significantly affects the reflected irradiance, with concrete being the most reflective under the same solar conditions. This aligns with findings from [44] and [16], who reported that high-albedo surfaces such as concrete and white-painted ground substantially increase rear-side contribution. The results further suggest that adjusting the tilt angle can moderately affect how much irradiance is reflected by different ground surfaces [17].

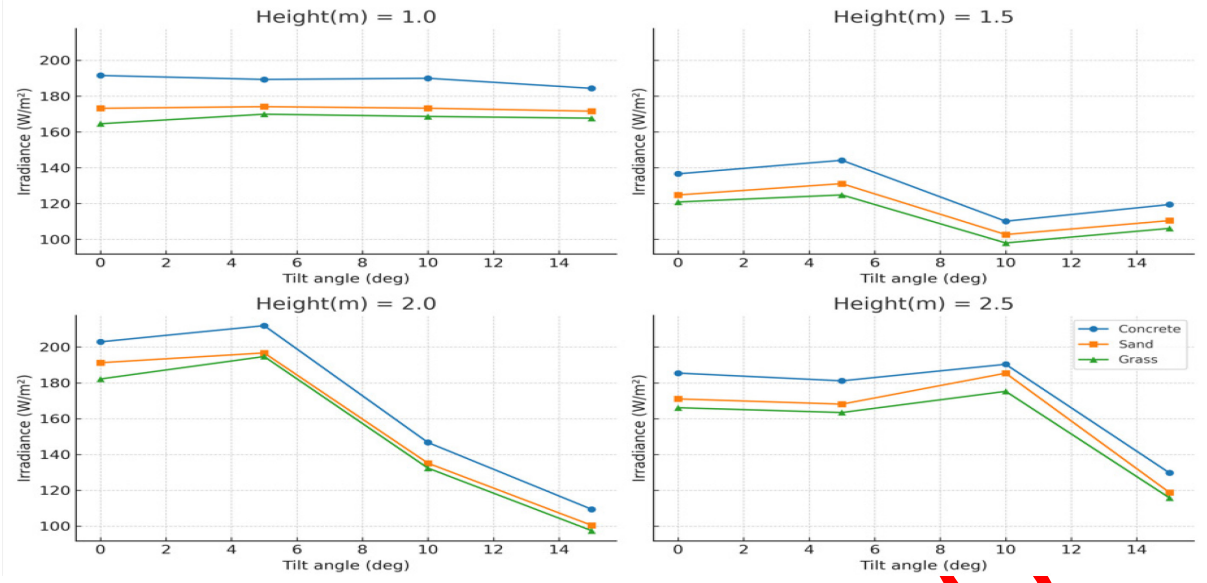

Figure 5:Reflected irradiance

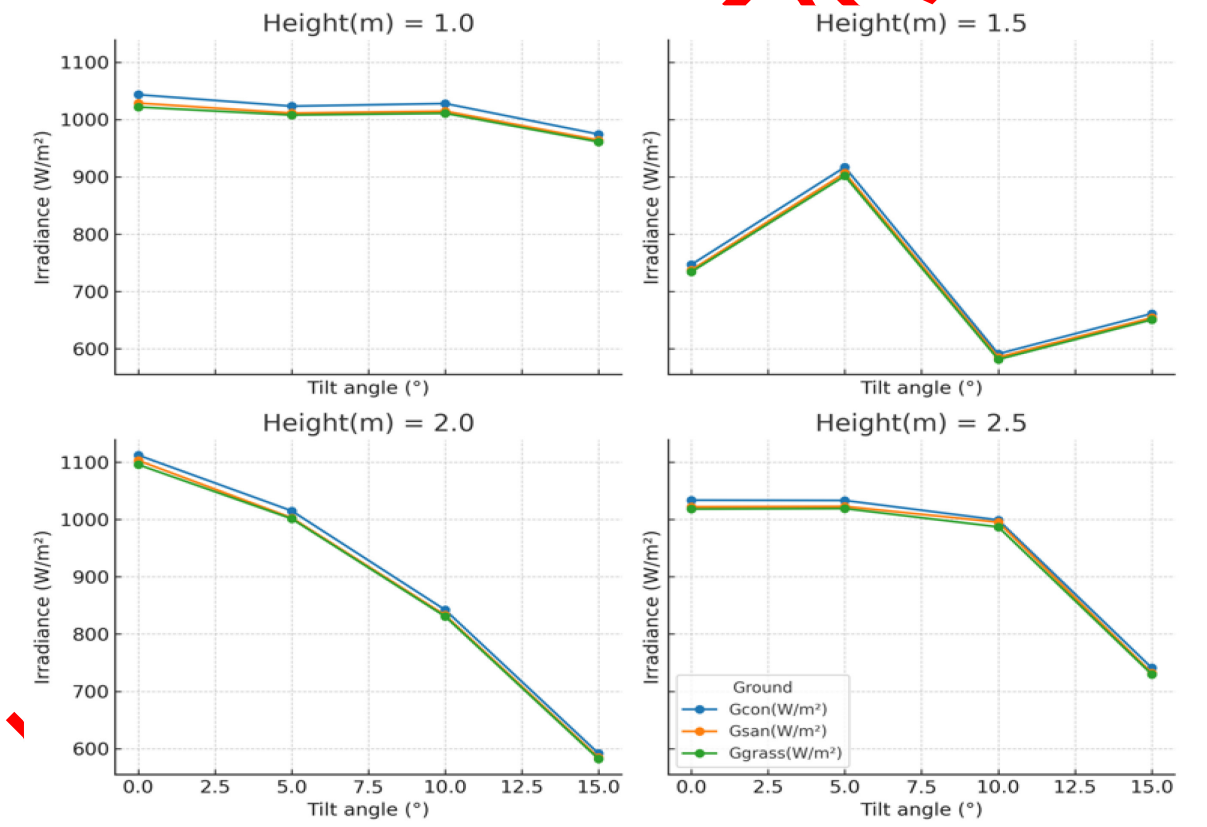

Figure 6:Total Irradiance received.

In Figure 6, the total irradiance received (Gcon, Gsan, and Ggrass) follows a similar trend across all surface types, indicating minimal variation due to surface material. The maximum total irradiance occurs at a 0° tilt angle, 2 m height, with the total irradiance from all surfaces exceeding 1000 W/m². The total irradiance is the combination of both incident and reflected irradiance. Optimizing the tilt angle enhances the solar irradiance captured. The minimum irradiance received is approximately 581 W/m². The total irradiance profiles seem to be similar regardless of surface

type, indicating that, although the nature of the surface has an effect on reflected irradiance, it exerts a limited effect on total irradiance absorbed by the panels.

Various surfaces, such as concrete, sand, and grass, have different albedo values that directly affect how much solar radiation is reflected. Albedo is the ratio of solar energy that is reflected from the ground surface back to the atmosphere and is an important factor in the local and global balance of energy [44]. In this study, concrete has an average albedo of 0.23, meaning it reflects 23 % of the incoming solar radiation. This characteristic of concrete means it has a very high reflectance compared to the other surface types analysed. The high albedo of concrete can thus increase the rear-side irradiance of bifacial solar panels, allowing for a larger portion of energy to be harvested.

Moderate albedo values are associated with dry and bright sand surfaces. In this experiment, the mean reflectance of sand was 0.21. While sand is less reflective than concrete, it does reflect a considerable amount of sunlight, so it is considered an "intermediate" surface for bifacial solar use, as shown in Figure 6. In contrast, grass and other similar types of vegetation have much lower albedo values. Grass surfaces had an average albedo of 0.19, meaning that grass absorbs more solar radiation and reflects less than concrete and sand. Grass surfaces, with a lower albedo, offered the least reflectance, confirming earlier observations in Malaysian [17] and Philippine [10] studies where vegetation-covered sites underperformed compared to high-reflectivity grounds. Although the disparity between sand and grass is minimal, grass tends to be more sand-like than concrete when it comes to reflectivity.

The total irradiation received by a bifacial solar panel is the combined contribution of front-side and rear-side irradiation. While the front side captures direct sunlight and diffuse sky radiation, the rear side primarily absorbs reflected radiation (albedo) from the ground and surrounding surfaces [32]. The total irradiance G_T received by the plane, as shown in Figure 6, can be expressed as using Equation 12.

Significance of Height

As shown in Table 7, panel elevation has a strong effect on energy production from bifacial solar panels according to the experimental data. Regardless of the type of surface, the energy production increased when the panels were elevated from 1 m to 2 m. This trend is attributable to enhanced rear-side irradiance capture at higher elevations, where self-shading is reduced and the rear surface maintains a larger, unobstructed view factor to reflective ground areas. Similar gains have been reported in tropical and subtropical settings by [16] and [31], who observed performance improvements of 10–20 % when elevating panels above 1.5 m, due to improved light collection and reduced ground shadowing.

Table 7: Average Energy Harvested at varying heights

Height(m)	Average Energy (KWh)		
	Concrete	Sand	Grass
1	12.2	12.1	11.9
1.5	12.5	12.3	12.1
2	14.2	14.0	13.9
2.5	13.8	13.5	13.4

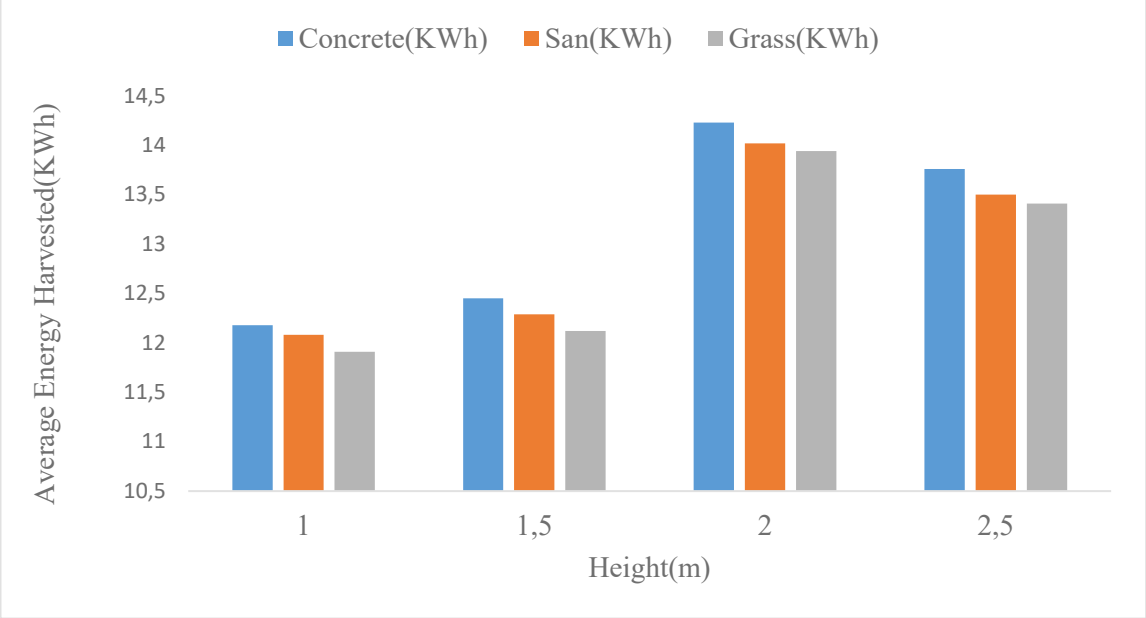

Figure 7: Energy harvested at different heights

From Figure 7, at 1m, all three surfaces recorded the lowest energy production, likely due to limited rear-side irradiance caused by proximity to the ground and increased shading. As height increased to 1.5 m, a moderate rise in energy output was noted, indicating improved irradiance exposure [11]. The experimental results showed that the highest energy output occurred at a height of 2 m. At this height, bifacial panels could capture the highest energy because there was little or no self-shading and also a larger angle of incidence for reflected light. As Table 7 shows, in concrete, the energy generated at a height of 1m was 12.2 kWh and 14.2 kWh at a height of 2 m, which represents an increase of around 16.8 %. This aligns closely with findings from [32] in tropical freshwater systems, where 2 m mounting maximized bifacial gain without incurring substantial structural complexity. When the height of the panel was increased to 2.5 m, the energy estimation slightly decreased. This indicates the beginning of the saturation effect, possibly due to higher exposure to wind or thermal losses that compensate more positively than the advantages of irradiance when the height increases, as also noted by [33].

These findings highlight that the installation height as well as the type of the installation surface should be carefully chosen in order to optimally exploit the energy harvesting potential of bifacial PV systems [9]. The mounting height of 2 m is identified as the most favourable mounting height for tropical regions, balancing irradiance capture with minimal performance losses. This height is where exposure to reflected and diffuse irradiance is optimal, and therefore, bifacial solar systems will be most productive.

From a deployment perspective, the findings have direct implications for utility-scale PV design in tropical regions. Adopting low tilt angles (around 5°) on high-albedo surfaces, combined with mounting heights of 2 m, can maximize bifacial energy yield while minimizing land use, installation complexity, and soiling issues. For large-scale projects, such configurations could reduce the levelized cost of electricity (LCOE) by increasing annual energy output without the added capital and maintenance costs of tracking systems.

CONCLUSIONS

This study investigated how tilt angle and mounting height affect the energy output of bifacial photovoltaic panels in tropical regions with high solar altitudes. Emphasizing the importance of location-specific irradiance models, it proposed fixed tilt angles as a cost-effective and scalable

alternative to dynamic tracking systems. Field tests were conducted using various surface types (concrete, sand, and grass), discrete tilt angles (0°, 5°, 10°, and 15°), and mounting heights (1.0–2.5 m). Results showed that moderate tilt angles between 5° and 10° offered the best trade-off between front-side irradiance capture and rear-side gains from ground reflection. A flat 0° tilt provided the highest front-side irradiance due to perpendicular alignment with the sun but lacked rear-side illumination and self-cleaning benefits. In contrast, steeper tilt angles beyond 10° caused notable efficiency losses due to angular misalignment with the sun's trajectory, estimated at approximately 5 %, 7 %, and 10 % for tilt angles of 5°, 10°, and 15°, respectively, compared to the 0° configuration. These findings highlight the need to balance increased ground-reflected irradiance with the cosine effect losses at higher tilts. Ultimately, the study concludes that a tilt angle of 5°, combined with optimized height and surface reflectivity, provides an ideal setup for maximizing energy output in bifacial PV systems within tropical environments.

Moreover, increasing panel height significantly improves rear-side irradiance and total energy yield, with the optimal performance recorded at a 2 m elevation, where the bifacial panel recorded an energy gain of approximately 16.8 %. Beyond this point, energy output declines slightly, suggesting that excessively high mounts offer a decrease in irradiation captured. Across all ground surfaces tested, concrete consistently yielded the highest energy due to its superior reflectivity.

The integration of simulation and experimental results revealed strong agreement, evidenced by a high correlation (r = 0.9681) and low error margins, validating the robustness of the models used. This synergy between theoretical modelling and empirical data strengthens the reliability of the optimization framework developed in this study.

From a broader perspective, the findings have important implications for utility-scale PV deployment in tropical regions. Implementing low tilt angles (around 5°), mounting heights of 2 m, and high-reflectivity surfaces such as concrete can significantly enhance bifacial panel performance while avoiding the costs and complexities of tracking systems. These design strategies not only maximize energy output but also reduce land-use intensity and lower the levelized cost of electricity (LCOE), making bifacial PV technology more viable for sustainable energy transitions in tropical developing nations.

ACKNOWLEDGMENT(S)

This study was supported by the German Academic Exchange Service (DAAD). This program would not have been possible without their generous support. The authors also express their gratitude to the entire staff of IEET, JKUAT, for their invaluable guidance and unwavering support during the research process.

NOMENCLATURE

Symbols

ρ	albedo
δ	declination angle
H	hour angle
γ	altitude
$\emptyset$	latitude
β	slope

Subscripts and superscrip

G_{POA}	Global plane of array
I_s	Solar constant
G_R	Reflected Irradiance
G_T	Total Irradiance

θ_z	Zenith Angle
V_{oc}	Open circuit voltage
I_{sc}	Short circuit current

Abbreviations

BF	Bifaciality factor
GHI	Global horizontal Irradiance
PV	Photovoltaic
DNI	Direct Normal Irradiance
DHI	Diffused horizontal irradiance
FF	Fill factor
GCR	Grand cover ratio
RCon	Reflected Irradiance from Concrete
RSand	Reflected Irradiance from Sand
RGrass	Reflected Irradiance from Grass
Vmpp	Voltage at Maximum Power Point
Impp	Current at Maximum Power Point
MPPT	Maximum power point tracking

REFERENCES

1. B. G. A Chathuranga, K. W. R. S. Premachandra, G. Sujeewan, J. D. R. R. Rathwaththa, P. A. I. S. Abejeewa, H.V.V. Priyadarshana, K.R. Koswattage, "A Comparative Experimental Performance Analysis for Fixed Solar PV Systems and Solar Tracker PV Systems in a Tropical Region," *International Journal of Research and Innovation in Applied Science*, vol. 9, no. 9, pp. 476–480, 2024, [online]. Available: https://ideas.repec.org/a/bjf/journl/v9y2024i9p476-480.html
2. T. Reindl, J. Ouyang, A. M. Khaing, K. Ding, Y. S. Khoo, T. M. Walsh, A. G. Aberle, "Investigation of the Performance of Commercial Photovoltaic Modules under Tropical Conditions," *Japanese Journal of Applied Physics.*, vol. 51, no. 10S, pp. 10NF11, 2012, doi: 10.1143/JJAP.51.10NF11.
3 H. Masrur, M. L. Othman, H. B. Hizam, N. I Wahab, S. Z. Islam, T. Senjyu, "Determining Optimal Tilt Angle to Maximize the PV Yield," in *2020 IEEE International Conference on Power and Energy (PECon)*, pp. 219–223, 2020 doi: 10.1109/PECon48942.2020.9314455.
4. M. Makenzi, J. Muguthu, and E. Murimi, "Maximization of Site-Specific Solar Photovoltaic Energy Generation through Tilt Angle and Sun-Hours Optimization," *Journal of Renewable Energy*, vol. 2020, no. 1, pp. 8893891, 2020, doi: 10.1155/2020/8893891.
5. M. Taha and S. Hameed, "Optimization of Tilt Angle of a PV System to Get Maximum Generated Power: a Case Study," *Kurdistan Journal of Applied Research*, vol. 5, no. 2, 2020, doi: 10.24017/science.2020.2.7.

6. C. E. Valdivia, C. T. Li, A. Russell, J. E. Haysom, R. Li, D. Lekx, M. M. Sepeher, D. Henes, K. Hinzer, H. P. Schriem, "Bifacial Photovoltaic Module Energy Yield Calculation and Analysis," in *2017 IEEE 44th Photovoltaic Specialist Conference (PVSC)*, pp. 1094–1099, 2017, doi: 10.1109/PVSC.2017.8366206.
7. O. H. AL-Zoubi, H. Al-Tahaineh, R. A. Damseh, A. H. AL-Zubi, A.-S. A. Odat, and B. Shboul, "Evaluating the real-world performance of vertically installed bifacial photovoltaic panels in residential settings: empirical findings and implications," *International Journal of Low-Carbon Technologies*, vol. 19, pp. 386–442, 2024, doi: 10.1093/ijlct/ctad138.
8. S. Bhaduri and A. Kottantharayil, "Mitigation of Soiling by Vertical Mounting of Bifacial Modules," *IEEE Journal of Photovoltaics*, vol. 9, no. 1, pp. 240–244, 2018, doi: 10.1109/JPHOTOV.2018.2872555.
9. R. A. Borea, V. Cirimele, F. Lo Franco, G. Maugeri, and F. Melino, "Impact of Environmental Variables on Tilt Selection for Energy Yield Maximization in Bifacial Photovoltaic Modules: Modeling Review and Parametric Analysis," *Applied Sciences*, vol. 14, no. 24, 2024, doi: 10.3390/app142411497.
10. I. B. Benitez, K. I. Repedro, and J. A. Principe, "Assessment of Solar PV Output Performance with Varying Tilt Angles and Weather Data from Era5: Case of Muntinlupa City, Philippines," *The International Archives of the Photogrammetry, Remote Sensing and Spatial Information Sciences*, vol. XLVIII-4-W8-2023, pp. 47–52, 2024, doi: 10.5194/isprs-archives-XLVIII-4-W8-2023-47-2024.
11. A. Manasrah, M. Masoud, Y. Jaradat, and I. Jannoud, "Advancements in Bifacial Photovoltaics: A Review of Machine Learning Techniques for Enhanced Performance," *ResearchGate*, vol. 27, pp. 239–245, 2024, doi: 10.55549/epstem.1518792.
12. S. Soulayman, "Optimum Tilt Angle and Maximum Possible Solar Energy Gain at High Latitude Zone," *Journal of Solar Energy Research*, vol. 1, no. 2, pp. 25–35, 2016, doi: 10.22059/JSER.2016.62297.
13. Y. B. Gebremedhen, "Determination of optimum fixed and adjustable tilt angles for solar collectors by using typical meteorological year data for Turkey," *International Journal of Renewable Energy Research*, vol. 4, no. 4, pp. 924–928, 2014, [online]. Available: https://dergipark.org.tr/en/pub/ijrer/issue/16073/168029
14. D. G. Qiu and S. B. Riffat, "Optimum tilt angle of solar collectors and its impact on performance," *International Journal of Ambient Energy*, vol. 24, no. 1, pp. 13–20, 2003, doi: 10.1080/01430750.2003.9674898.

15. S. Z. Issaq, S. Tala, and A. A. Azooz, "Empirical modeling of optimum tilt angle for flat solar collectors and PV panels | Request PDF," *Springer Nature link,* vol. 30, pp. 81250–81266, 2022, doi: 10.1007/s11356-023-28142-3.
16. D. L. R. García, M. Á. Muñoz Maldonado, Y. A. Acevedo Arenas, and J. Sebastián, "Evaluation of the impact of the main parameters affecting energy performance in bifacial photovoltaic modules in a tropical location.," in *LACCEI,* vol. 1, no. 8, 2023, doi: 10.18687/LACCEI2023.1.1.937.
17. M. N. Khai, N. M. Adam, O. Inayatullah, and Z. Kadir, "Assessment of solar radiation on diversely oriented surfaces and optimum tilts for solar absorbers in Malaysian tropical latitude," *Springer Nature link*, vol. 5, no. 1, 2014, doi: 10.1007/s40095-014-0075-7.
18. C. Oko and S. N. Nnamchi, "Optimum Collector Tilt Angles for Low Latitudes," *The Open Renewable Energy Journal*, vol. 5, no. 1, pp. 7–14, 2012, doi: 10.2174/1876387101205010007.
19. Solar PV potential in Kenya by locations, https://profilesolar.com/countries/KE/, [Accessed: 22-May-2025].
20. N. Mukisa and R. Zamora, "Optimal tilt angle for solar photovoltaic modules on pitched rooftops: A case of low latitude equatorial region," *Sustainable Energy Technologies and Assessments*, vol. 50, pp. 101821, 2022, doi: 10.1016/j.seta.2021.101821.
21. C. T. Warburg, T. Pogrebnaya, and T. Kivevele, "Optimized Tilted Solar Radiation in Equator Region: Case Study of Seven Climatic Zones in Tanzania," *Renewable Energy Research and Applications*, vol. 6, no. 1, pp. 75–82, 2025, doi: 10.22044/rera.2024.13606.1252.
22. S. Soulayman and W. Sabbagh, "Optimum Tilt Angle at Tropical Region," *Int. Journal of Renewable Energy Development (IJRED)*, vol. 4, no. 1, pp. 48-54, 2024, doi: 10.14710/ijred.4.1.48-54.
23. H. O. Njoku, U. G. Azubuike, E. C. Okoroigwe, and V. Ekechukwu, "Tilt angles for optimizing energy reception by fixed and periodically adjusted solar-irradiated surfaces in Nigeria," *Springer Nature link*, vol. 4, no. 8, pp. 437-452, 2020, doi: 10.1007/s42108-020-00072-7.
24. A. Eke and P. Etim, "Prediction of optimum tilt angle of Flat-plate solar collector in Abia State Nigeria," *International Journal of Engineering and Innovative Research*, vol. 4, no. 3, pp. 143–153, 2022, doi: 10.47933/ijeir.1000262.
25. N. Sharma, P. K. Tiwari, G. Ahmad, and H. Sharma, "Optimum Tilt and Orientation Angle Determination with Application of Solar data," in *2021 International Conference on*

Artificial Intelligence and Smart Systems (ICAIS), pp. 477–481, 2021 doi: 10.1109/ICAIS50930.2021.9395845.

26. B. R. Elhab, K. Sopian, S. Mat, C. Lim, M. Y. Sulaiman, M.H. Ruslan, O. Saadatian, "Optimizing tilt angles and orientations of solar panels for Kuala Lumpur, Malaysia," *Scientific Research and Essays*, vol. 7, no. 42, pp. 3758–3765, 2012, doi: 10.5897/SRE12.241.
27. D. Machidon and M. Istrate, "Tilt Angle Adjustment for Incident Solar Energy Increase: A Case Study for Europe," *Sustainability*, vol. 15, no. 8, pp. 7015, 2023, doi: 10.3390/su15087015.
28. D. Solyali and A. Mollaei, "A Simulation Model Based on Experimental Data to Determine the Optimal Tilt Angle for a Fixed Photovoltaic Panel," *Archives of Advanced Engineering Science*, vol. 3, no. 1, 2025, doi: 10.47852/bonviewAAES3202907.
29. A. Asgharzadeh, B. Marion, C. Deline, C. Hansen, J. S. Stein, and F. Toor, "A Sensitivity Study of the Impact of Installation Parameters and System Configuration on the Performance of Bifacial PV Arrays," *IEEE Journal of Photovoltaics*, vol. 8, no. 3, pp. 798–805, 2018, doi: 10.1109/JPHOTOV.2018.2819676.
30. A. Asgharzadeh, T. Lubenow, J. Sink, B. Marion, C. Deline, C. Hansen, J. Hansen, F. Toor, "Analysis of the Impact of Installation Parameters and System Size on Bifacial Gain and Energy Yield of PV Systems," in *2017 IEEE 44th Photovoltaic Specialist Conference (PVSC)*, pp. 3333–3338, 2017, doi: 10.1109/PVSC.2017.8366690.
31. A. H. Salum, O. A. Abdulrazzaq, A. Y. Qasim, B. H. Ismail, and S. M. Awad, "Determination of Optimal Elevation of Silicon Bifacial Solar Panel," *Iraqi Journal of Industrial Research*, vol. 9, no. 1, 2022, doi: 10.53523/ijoirVol9I1ID147.
32. G. R. Pandian, G. B. Balachandran, P. W. David, and S. K, "Performance analysis of floating bifacial stand-alone photovoltaic module in tropical freshwater systems of Southern Asia: an experimental study," *Scientific Reports*, vol. 14, article no. 20352, 2024, doi: 10.1038/s41598-024-70015-3.
33. C. Zhang, H. Shen, and H. Liu, "The Influence of the Installation Condition and Performance of Bifacial Solar Modules on Energy Yield," *Energies*, vol. 16, no. 21, pp. 7396, 2023, doi: 10.3390/en16217396.
34. G. Y. Kim, D. S. Han, and Z. Lee, "Solar Panel Tilt Angle Optimization Using Machine Learning Model: A Case Study of Daegu City, South Korea," *Energies*, vol. 13, no. 3, 2020, doi: 10.3390/en13030529.
35. O. Francis, L. Olang, and J. Strobl, "Spatial Modelling of Solar Energy Potential in Kenya," 2017, [Online]. Available: http://hdl.handle.net/123456789/1706

36. B. M. Abdoulaye, H. S. Ousmane, S. D. N. Harouna, and B. Makinta, "A Comparative Study of Two Common Software's used for Photovoltaic Systems, RETscreen and PVsyst," *CJAST*, vol. 43, no. 5, pp. 11–18, 2024, doi: 10.9734/cjast/2024/v43i54373.
37. S. Satheesh, S. Venkat, and R. B. Mulford, "Optimization of Panel Spacing, Tilt Angle and Azimuth Angle for Bifacial Panels with Fixed Land Acreage and Orientation for Several United States Locations,"*ASME,PP. 9, 2024,* doi: 10.1115/ES2024-131110.
38. P. Headley, "A Method for Calculating the Equation of Noon (an English translation of Methodus Computandi Aequationem Meridiei)," *Euleriana*, vol. 2, no. 2, pp. 67–78, 2022, doi: 10.56031/2693-9908.1034.
39. O. Chikere Aja, H. H. Al-Kayiem, and Z. Ambri Abdul Karim, "Analytical investigation of collector optimum tilt angle at low latitude," *Journal of Renewable and Sustainable Energy*, vol. 5, no. 6, pp. 063112, 2013, doi: 10.1063/1.4829434.
40. R. O. Yakubu, L. D. Mensah, D. A. Quansah, and M. S. Adaramola, "Improving solar photovoltaic installation energy yield using bifacial modules and tracking systems: An analytical approach," *Advances in Mechanical Engineering*, vol. 14, no. 12, pp. 1-12, 2022, doi: 10.1177/16878132221139714.
41. T. Mahachi and A. J. Rix, "Evaluation of irradiance decomposition and transposition models for a region in South Africa Investigating the sensitivity of various diffuse radiation models," in *IECON 2016 - 42nd Annual Conference of the IEEE Industrial Electronics Society*, pp. 3064–3069, 2016, doi: 10.1109/IECON.2016.7793897.
42. S. Guo, T. M. Walsh, and M. Peters, "Vertically mounted bifacial photovoltaic modules: A global analysis," *Energy*, vol. 61, pp. 447–454, 2013, doi: 10.1016/j.energy.2013.08.040.
43. M. Lave, W. Hayes, A. Pohl, and C. W. Hansen, "Evaluation of Global Horizontal Irradiance to Plane-of-Array Irradiance Models at Locations Across the United States," *IEEE Journal of Photovoltaics*, vol. 5, no. 2, pp. 597–606, 2015, doi: 10.1109/JPHOTOV.2015.2392938.
44. H. Kathuria, I. Singh, A. Gupta, G. Puniya, and B. Kumar, "Analysis of Bifacial Photovoltaic Panel Under Different Reflective Surfaces," in *2024 IEEE Third International Conference on Power Electronics, Intelligent Control and Energy Systems (ICPEICES)*, pp. 933–938, 2024, doi: 10.1109/ICPEICES62430.2024.10719302.
45 H. Hosamo and S. Mazzetto, "Performance Evaluation of Machine Learning Models for Predicting Energy Consumption and Occupant Dissatisfaction in Buildings," *Buildings*, vol. 15, no. 1, pp. 39, 2025, doi: 10.3390/buildings15010039.

46. Q. Chen, Z. Cai, Y. Han, M. Zhang, B. Li, and L. Luo, "Study on the effect of PV tilt angle on power generation," *J. Phys.: Conf. Ser.*, vol. 2771, no. 1, pp. 012027, 2024, doi: 10.1088/1742-6596/2771/1/012027.
47. E. C. Obuah and Tamuno-Omie Joyce Alalibo, "Effect of Change in Tilt Angle on the Performance of Photovoltaic Systems," vol. 66, no. 1, pp. 13–22, 2020, doi: 10.5281/ZENODO.3614866.
48. S. Ghosh, J. N. Roy, and C. Chakraborty, "Maximizing PV generation with lower tilt angles to meet high summer electricity demand on the Indian electricity grid," *Energy for Sustainable Development*, vol. 80, pp. 101446, 2024, doi: 10.1016/j.esd.2024.101446.
49 J. Freeman, J. Whitmore, N. Blair, and A. P. Dobos, "Validation of multiple tools for flat plate photovoltaic modeling against measured data," in *2014 IEEE 40th Photovoltaic Specialist Conference (PVSC)*, pp. 1932–1937, 2014, doi: 10.1109/PVSC.2014.6925304.
50 M. Coello and L. Boyle, "Simple Model For Predicting Time Series Soiling of Photovoltaic Panels," *IEEE Journal of Photovoltaics*, vol. 9, no. 5, pp. 1–6, 2019, doi: 10.1109/JPHOTOV.2019.2919628.
51 A. Driesse and J. S. Stein, "Global normal spectral irradiance in Albuquerque: a one-year open dataset for PV research," *Sandia National Laboratories*, 2020, Accessed: Sep. 12, 2025. [Online]. Available: https://www.osti.gov/servlets/purl/1814068
52 J. A. Duffie, W. A. Beckman, and N. Blair, *Solar Engineering of Thermal Processes, Photovoltaics and Wind*. John Wiley & Sons, 2020.
53 J . S. Haberl, C. Culp, and D. E. Claridge, "ASHRAE's Guideline 14-2002 for Measurement of Energy and Demand Savings: How to Determine What Was Really Saved by the Retrofit," ResearchGate, https://www.researchgate.net/publication/26901656_ASHRAE's_Guideline_14-2002_for_Measurement_of_Energy_and_Demand_Savings_How_to_Determine_What_Was_Really_Saved_by_the_Retrofit, [Accessed: 05-Sep- 2025].
54 A. Radwan, A. Mdallal, S. Haridy, M. A. Abdelkareem, A. H. Alami, and A. G. Olabi, "Optimizing the annual energy yield of a residential bifacial photovoltaic system using response surface methodology," *Renewable Energy*, vol. 222, pp. 119914, 2024, doi: 10.1016/j.renene.2023.119914.